THE JOURNAL OF PHYSICAL CHEMISTRY Letters

Letter

pubs.acs.org/JPCL

Enhanced Electrocatalytic Properties of Transition-Metal Dichalcogenides Sheets by Spontaneous Gold Nanoparticle Decoration

Jaemyung Kim,[†] Segi Byun,[†,‡] Alexander J. Smith,[†] Jin Yu,[‡] and Jiaxing Huang*[,†]

[†]Department of Materials Science and Engineering, Northwestern University, Evanston, Illinois 60208, United States

[‡]Department of Materials Science and Engineering, Korea Advanced Institute of Science and Technology, Daejeon 305-701, Republic of Korea

Supporting Information

ABSTRACT: Here, we report that transition-metal dichalcogenides such as MoS_2 and WS_2 can be decorated with gold nanoparticles by a spontaneous redox reaction with hexachloroauric acid in water. The resulting gold nanoparticles tend to grow at defective sites, and therefore, selective decorations at the edges and the line defects in the basal planes of bulk single crystals were observed. The lithium intercalation−exfoliation process makes the basal planes of chemically exfoliated MoS_2 and WS_2 sheets much more defective than their single-crystalline counterparts, leading to a more uniform and higher-density deposition of gold nanoparticles. Due to the greatly improved charge transport between adjacent sheets, the resulting MoS_2/Au and WS_2/Au hybrids show significantly enhanced electrocatalytic performance toward hydrogen evolution reactions.

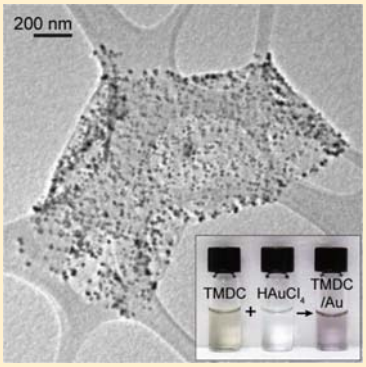

SECTION: Energy Conversion and Storage; Energy and Charge Transport

Two-dimensional (2D) sheets exfoliated from bulk layered inorganic compounds, such as transition-metal dichalcogenides (TMDC) MoS_2 and WS_2, have gained wide attention in recent years as graphene analogues with interesting electronic, optical, mechanical, and catalytic properties.[1] Although significant efforts have been made on the investigation of the electronic and optical properties of single- or few-layered TMDCs,[1−3] interest in the chemical properties and surface functionalization of these 2D sheets has only recently started to emerge. As has been extensively shown with graphene-based materials, decorating the sheets with nanoparticles is an effective way to functionalize the surface and render new and enhanced properties for areas such as energy storage and catalysis.[4−11] Several strategies have been demonstrated to decorate TMDC with metal nanoparticles.[12−17] Typically, this has been done by either simply mixing the individual constituents[12,13] or adding the TMDC sheets in the reaction between the metal precursors and reducing agents, depositing the nanoparticles in situ onto the sheets.[15,16] Because TMDC compounds have rich redox chemistry, however, they themselves could directly react with metal precursors to allow a very straightforward and clean synthesis of metal-decorated sheets.

TMDC compounds, especially MoS_2 and WS_2, are emerging electrocatalysts for hydrogen evolution reactions (HERs).[18−21] Recently, HERs catalyzed by chemically exfoliated TMDC layers were reported.[22,23] Significantly, evidence suggests that chemically exfoliated TMDC sheets have advantages over synthesized sheets because the highly strained 1T phases existing on the single layers could help to lower the overpotential needed for HERs.[23] A challenge with using the chemically exfoliated TMDC sheets is their tendency to restack during materials processing, which will not only hinder the vertical charge transport but also limit the accessibility of protons to the catalytically active sites of TMDC. These problems may be addressed by decorating the sheets with electrically conductive metal nanoparticles, such as Au, which could enhance the charge transport along interplanar directions and act as spacers to inhibit restacking. The use of high-cost materials such as gold can be justified if the amount needed is small compared to the TMDC.

Herein, we report spontaneous decoration of Au nanoparticles on MoS_2 and WS_2 sheets upon direct reaction with a gold precursor hexachloroauric acid ($HAuCl_4$) in water. The decoration reaction occurs on the surface of both bulk TMDC single crystals and chemically exfoliated sheets. The presence of Au nanoparticles on chemically exfoliated MoS_2 and WS_2 nanosheets greatly improves charge transport between the sheets and enhances their HER catalytic efficiency.

When a piece of single-crystalline MoS_2 is immersed into an aqueous solution of $HAuCl_4$ (typical concentration of 1×10^{-3}

Received: March 6, 2013
Accepted: March 25, 2013

   dx.doi.org/10.1021/jz400507t | J. Phys. Chem. Lett. 2013, 4, 1227−1232

M), spontaneous reaction can occur, decorating the MoS_2 crystal with gold nanoparticles, as shown in the scanning electron microscopy (SEM) images shown in Figure 1.

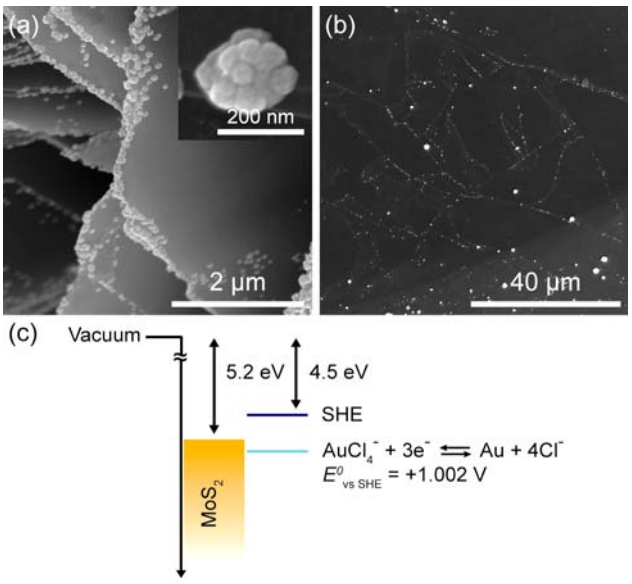

Figure 1. SEM images showing gold nanoparticles preferentially grown at defect sites such as (a) edges or (b) line defects on the basal plane of a MoS_2 single crystal after immersion in an aqueous solution of $HAuCl_4$. The inset in (a) shows a higher magnification image. (c) An energy diagram showing that the Fermi level of MoS_2 lies above the reduction potential of Au^{3+} (+1.002 V versus SHE). Therefore, a spontaneous redox reaction should occur between MoS_2 and $HAuCl_4$.

Notably, we found that the resulting gold nanoparticles preferentially decorate defect sites of MoS_2 single crystals, such as edges (Figure 1a) or line defects on the basal plane (Figure 1b), while the main basal plane remains largely unaffected on the microscopic scale. Previously, gold deposited by thermal evaporation was observed to preferentially nucleate at the defect sites of bulk MoS_2.[24] Spontaneous reduction of gold ions by carbon-based materials such as carbon nanotubes or graphene has also been observed.[25−27] Here, the underlying mechanism is also likely due to the redox reaction between MoS_2 and gold ions. The work function of MoS_2 is 5.2 eV,[28] situating the Fermi level of MoS_2 well above the reduction potential of $AuCl_4^-$ (+1.002 V versus the standard hydrogen electrode (SHE), Figure 1c).[29] Therefore, $MoS_2/AuCl_4^-$ should form a redox pair, allowing spontaneous electron transfer from MoS_2 to gold ions to occur and leading to the formation of gold nanoparticles. It follows that these gold nanoparticles would preferentially nucleate at the highly energetic defect sites such as edges or line defects. One may also expect a small portion of Mo atoms to be oxidized to water-soluble, higher valence forms and leached into the solution.

We found that the same reaction that occurs with bulk MoS_2 can occur with chemically exfoliated MoS_2 sheets. To prepare single layers of MoS_2, we employed the lithium intercalation−exfoliation approach developed by Morrison and co-workers.[30] After extensive purification, a stable colloidal dispersion of MoS_2 single-layered sheets dispersed in water can be obtained. The violent intercalation−exfoliation reactions produce high local strain, triggering a partial phase transformation from trigonal prismatic (2H) to octahedral (1T).[31,32] Therefore, one would expect such exfoliated sheets to become much more defective and reactive. Indeed, we noticed that some sheets produced by chemical exfoliation appear more defective even at the microscopic scale when observed under an atomic force microscope (AFM). Figure S1 (Supporting Information) shows AFM images contrasting the MoS_2 sheets obtained by chemical exfoliation and mechanical exfoliation from a single crystal. The chemically exfoliated sheets have jagged edges and sometimes even cracks in the basal plane, while the single layer produced by mechanical exfoliation shows sharp edges and a smooth surface. Therefore, we expect that chemically exfoliated MoS_2 sheets will have many more reactive sites, even in the basal planes, for gold decoration.

Figure 2a shows UV/vis absorption spectra of an aqueous dispersion of chemically exfoliated MoS_2 sheets, an aqueous

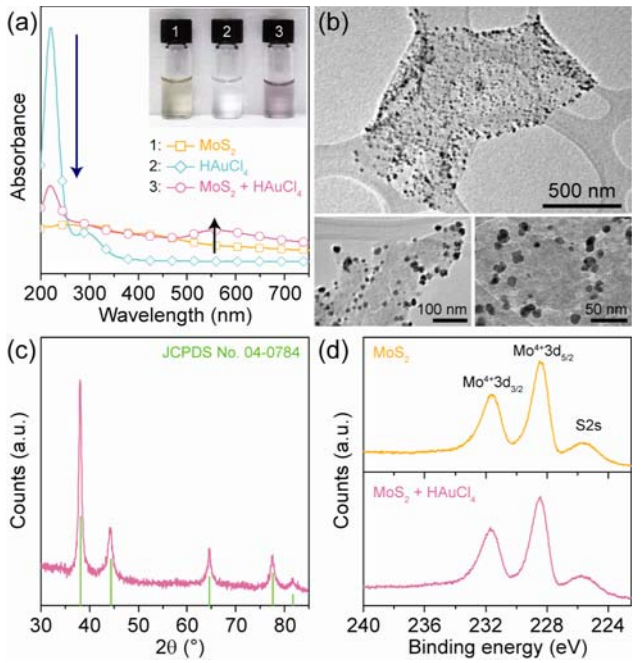

Figure 2. The rapid spontaneous reaction between chemically exfoliated colloidal MoS_2 and $HAuCl_4$ produces Au-decorated sheets. (a) UV/vis spectra of a MoS_2 dispersion (orange squares), $HAuCl_4$ solution (blue diamonds), and their mixture (magenta circles). Upon mixing, the $HAuCl_4$ peak diminishes, as indicated by the blue arrow, and a new absorption band at around 550 nm corresponding to Au nanoparticles emerges, as indicated by the black arrow. The photo in the inset shows the colors of MoS_2, $HAuCl_4$, and their mixture. (b) TEM images showing a MoS_2 sheet uniformly decorated by Au nanoparticles (top). On some sheets, Au nanoparticles can be seen preferentially nucleating along the cracks (bottom). (c) The XRD pattern of the product has strong diffraction peaks matching the standard diffraction pattern of gold (JCPDS 04-0784). (d) No significant Mo3d band shifts can be detected by XPS before (top) and after (bottom) gold decoration, suggesting that most of MoS_2 remains unoxidized upon the reaction.

solution of $HAuCl_4$, and a mixture of the two. When a small aliquot of $HAuCl_4$ was added into chemically exfoliated MoS_2, the absorption peak of the gold precursor at around 215 nm decreased significantly, while a new absorption peak corresponding to the Au plasmon band at around 550 nm emerged, suggesting the consumption of Au^{3+} and the formation of gold nanoparticles. Upon mixing, an obvious color change was observed as the dispersion changed from yellow to purple

dx.doi.org/10.1021/jz400507t | J. Phys. Chem. Lett. 2013, 4, 1227−1232

(Figure 2a, inset). The reaction occurred instantaneously and completed within seconds. Transmission electron microscopy (TEM) images of the chemically exfoliated MoS_2 sheets after the gold decoration show that unlike in the case of a single crystal (Figure 1), gold nanoparticles uniformly decorated both the edges and the basal planes of the MoS_2 single layers (Figure 2b, top). In some cases, the gold nanoparticles can be seen clearly following cracks in the basal plane of the sheets (Figure 2b, bottom), further suggesting that the gold nucleation preferentially occurs at defect sites. Figure S2 (Supporting Information) shows high-resolution TEM (HRTEM) images of gold nanoparticles on MoS_2. The particles do not appear to be single-crystalline, similar to what was observed in a recent report.[17] X-ray diffraction (XRD) (Figure 2c) and X-ray photoelectron spectroscopy (XPS) studies (Figure S3, Supporting Information) confirmed that the gold precursor was indeed reduced. XPS data exhibit no significant shift in Mo3d bands before and after gold decoration (Figure 2d). A Raman spectrum obtained from a sample drop-casted on a Si substrate showed strong E^1_{2g} and A_{1g} bands of MoS_2 at 383 and 408 cm^{-1}, respectively (Figure S4, Supporting Information), suggesting that most of MoS_2 in the hybrid material remains unoxidized. However, when a significant molar fraction of gold was incorporated into MoS_2 (>60 mol %), a more significant contribution from Mo^{6+} $3d_{3/2}$ at around 236 eV and Mo^{6+} $3d_{5/2}$ at around 232 eV could be observed (Figure S5, Supporting Information) in XPS spectra, suggesting the oxidation of MoS_2 to molybdic acid.

The density and size of the gold nanoparticles decorating the MoS_2 sheets can be easily tuned by controlling the amount of $HAuCl_4$ added into the dispersion. For instance, we observed a red shift in the UV/vis spectra of MoS_2/Au hybrids by gradually increasing the molar concentration of $HAuCl_4$ added into the MoS_2 dispersions of a fixed concentration (Figure S6, Supporting Information), indicating the formation of larger gold nanoparticles. This was also confirmed by the TEM images shown in Figure S7 (Supporting Information). The extent of gold ion reduction by the spontaneous redox reaction can be estimated by monitoring the UV/vis absorption peak of Au^{3+} at around 215 nm before and after the reaction, which can be used to quantify the loading level of Au in the final MoS_2/Au hybrid.

TMDCs, most notably MoS_2 and WS_2, have recently gained much interest as promising electrocatalysts for hydrogen evolution.[18,19,33,34] Their catalytic efficiency, however, is limited by inherently low interparticle conductivity between adjacent van der Waals bonded sheets.[18] Au decoration of MoS_2 sheets should therefore greatly improve the charge transport between neighboring sheets, leading to enhanced electrocatalytic performances. Previous density functional theory studies suggested that only one-quarter of the edge sites contribute to the H_2 evolution at a given time.[35,36] Because the reduced Au atoms segregated into nanoparticles on the edge, Au decoration is unlikely to cause significant blockage of the active edge sites, especially at a low loading level.

HER measurements were therefore undertaken with a standard three-electrode setup in 0.5 M H_2SO_4 (see Experimental Methods) to assess the influence of the Au nanoparticles on MoS_2's electrocatalytic behavior. Figure 3a shows polarization curves of the MoS_2/Au hybrids with increasing molar loading levels of gold. As the amount of gold nanoparticles increases, the overpotential (η) decreases, while the current density (j) increases, exhibiting higher HER

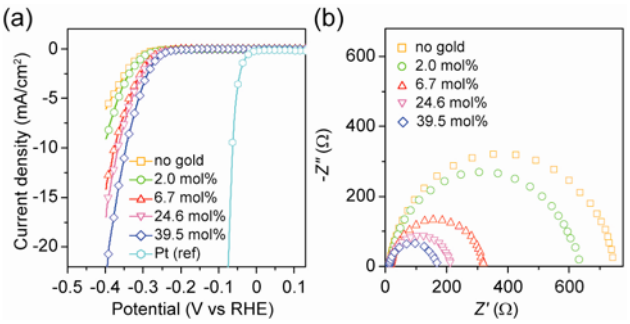

Figure 3. Electrocatalytic HER performance of MoS_2/Au. (a) As the loading level of gold increases, the overpotential decreases, while the current density increases, likely due to the enhanced charge transport in the interplanar direction (b), as suggested by greatly decreased charge-transport impedance (Z').

electrocatalytic performance compared to that of the bare chemically exfoliated MoS_2 sheets. The overpotential values of bare MoS_2 reported here are much lower compared to previously reported values for chemically exfoliated MoS_2 sheets.[22] The Tafel slopes (b) estimated from the linear portions of Tafel plots (not shown) also gradually decreased from 65.53 to 56.97 mV/dec as the molar percentages of gold incorporated into MoS_2 were increased from 0 to 39.5%, respectively, leading to the higher current densities at the same overpotential with gold decoration. Impedance measurements performed on the same samples (Figure 3b) show that the charge-transport impedance (Z') was significantly reduced by incorporating even a very small amount (3.3 mol %) of gold, suggesting that the observed HER performance enhancement originates from improved charge transport through the gold nanoparticles. The overpotentials, current densities, Tafel slopes, and charge-transport impedances of MoS_2 with varying amounts of gold incorporation are summarized in Table 1.

Table 1. Summary of HER Performance Parameters of MoS_2 Sheets Decorated with Varying Amounts of Gold Nanoparticles

Au (mol %)	η (V)	$j_{\eta=0.4\ V}$[a] (mA/cm²)	b (mV/dec)	Z' (Ω)
0	0.252	6.08	65.53	738
2.0	0.242	9.08	64.53	623
6.7	0.223	14.14	58.97	315
24.6	0.219	16.99	56.98	207
39.5	0.205	22.62	56.97	162

[a]Current densities at η = 0.4 V.

Because WS_2 exhibits very similar electronic, optical, and chemical properties to MoS_2, we found that the gold decoration chemistry also works with WS_2, which has a work function of 5.1 eV.[37] Adding a small aliquot of $HAuCl_4$ solution into an aqueous dispersion of chemically exfoliated WS_2 sheets can also result in spontaneous Au decoration (Figure 4a, inset). UV/vis spectra in Figure 4a show that upon reaction, the absorption peak of Au^{3+} at around 215 nm significantly decreased, while the new band corresponding to Au nanoparticles at around 550 nm started to appear. A TEM image of the sample also confirmed the successful decoration of gold nanoparticles onto WS_2 sheets (Figure 4b), similar to the case of MoS_2 (Figure 2b). As with MoS_2, Au decoration also enhances the HER activity of WS_2 sheets (Figure 4c), as well as the charge-

dx.doi.org/10.1021/jz400507t | J. Phys. Chem. Lett. 2013, 4, 1227−1232

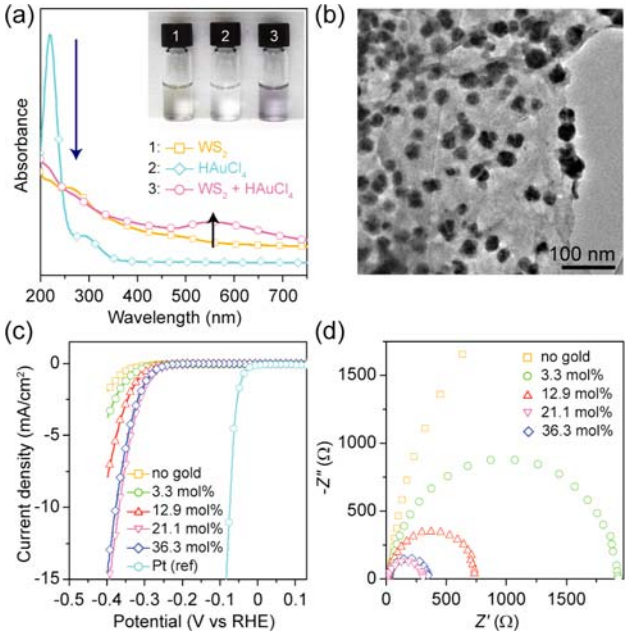

Figure 4. Spontaneous decoration of gold nanoparticles on chemically exfoliated WS_2 sheets. (a) As in the case of MoS_2, $HAuCl_4$ is consumed upon reacting with WS_2 to produce gold nanoparticles, as indicated by a new absorption band at around 550 nm and the color change of the dispersion from yellow to purple (inset). (b) TEM image showing gold nanoparticles uniformly decorating a WS_2 sheet. (c) Polarization curves and (d) impedance spectra showing enhanced electrocatalytic HER performance of WS_2 sheets and reduced charge-transport impedance, respectively, upon gold decoration.

transport impedance (Figure 4d). Compared to MoS_2, gold decoration of WS_2 resulted in an even more significant enhancement in HER activity and a reduction in charge-transport impedance, especially at low loading level. This may be attributed to the lower initial electrical conductivity of the chemically exfoliated WS_2. For both MoS_2 and WS_2, the Li intercalation−exfoliation process induces a partial phase transition of the sheets from the semiconducting 2H phase to metallic 1T phase. Becuase it is more difficult to intercalate Li into WS_2 than MoS_2,[38] we postulate that the Li intercalation−exfoliation was less effective for WS_2 in our experiments, leading to a lower degree of 2H to 1T phase transition. This would result in a lower initial conductivity due to a smaller fraction of the more conducting 1T phase and would lead to a larger value of initial charge-transport impedance. Hence, a small degree of gold decoration (3.3 mol %) could result in over 25% improvement in electron transport of the hybrid material. Furthermore, less effective Li intercalation should result in a smaller density of catalytically reactive sites in the chemically exfoliated WS_2 sheets. As a result, decreased HER efficiency of the WS_2/Au hybrid can be observed at high loading level of Au (>30 mol %) (Figure S8, Supporting Information), suggesting that a significant portion of the active sites are blocked by Au. This suggests that the main contribution of Au nanoparticles is to promote the charge transport between adjacent layers. The HER performance parameters of WS_2 with varying amounts of gold incorporation are summarized in Table 2.

In summary, we demonstrated that MoS_2 and WS_2 can be decorated with gold nanoparticles by a spontaneous redox reaction between the TMDC compounds and hexachloroauric

Table 2. Summary of HER Performance Parameters of WS_2 Sheets Decorated with Varying Amounts of Gold Nanoparticles

Au (mol %)	η (V)	$j_{\eta=0.4\ V}$[a] (mA/cm²)	b (mV/dec)	Z' (Ω)
0	0.282	1.91	110.28	7500
3.3	0.264	3.72	80.79	1909
12.9	0.247	7.91	66.67	735
21.1	0.23	15.67	56.69	292
36.3	0.233	14.5	57.49	335

[a]Current densities at η = 0.4 V.

acid in water. The resulting gold nanoparticles tend to grow at the defective sites of the sheets. The chemical intercalation−exfoliation process makes the basal plane of the sheets much more defective than their single-crystalline counterparts, thus resulting in a higher-density deposition of Au nanoparticles. The resulting MoS_2/Au and WS_2/Au hybrids show significantly enhanced electrocatalytic performance toward HER, which is attributed to greatly improved charge transport between neighboring sheets, as indicated by reduced charge-transport impedance. Au-decorated TMDC sheets could become a base material for exploring surface-plasmon-enhanced photo- and electrocatalysts for the oxidation of organic molecules or HER.[39,40] With abundant chemistry available for transition-metal compounds, chemically exfoliated TMDC sheets should be versatile platforms for constructing highly functional inorganic 2D systems.

■ EXPERIMENTAL METHODS

All chemicals except for MoS_2 single crystals (SPI Supplies) were purchased from Sigma-Aldrich. To make chemically exfoliated MoS_2 single layers, MoS_2 powder was stirred in a 1.6 M solution of *n*-butyllithium in hexane for 2 days in a N_2-filled glovebox, followed by a reaction with water outside of the glovebox and extensive purification steps. In the case of WS_2, Li was intercalated by a solvothermal method, as previously reported.[41] To decorate TMDC with gold nanoparticles, a small aliquot of $HAuCl_4$ solution in water was added into an aqueous dispersion of chemically exfoliated MoS_2 or WS_2 at room temperature. The reaction occurred instantaneously and completed within seconds. SEM and TEM images were taken on an FEI Nova 600 SEM and a JEOL 2100F TEM, respectively. AFM images were taken on a Park Systems XE-100 under tapping mode. UV/vis absorption spectra were measured with an Agilent 8653 UV/vis spectrometer. XRD patterns were obtained on a Rigaku D/Max powder diffractometer with Cu Kα radiation, and Raman spectroscopy was performed using a WITec Alpha 300 system with an excitation wavelength of 532 nm. XPS spectra were recorded on a Thermo Scientific ESCALAB 250Xi. Electrocatalytic measurements were performed using an AUTOLAB PGASTAT 302N potentiostat with a standard three-electrode setup in 0.5 M H_2SO_4 (scan rate = 5 mV/s). Working electrodes were prepared by drop-casting the samples on a glassy carbon electrode, and a graphite rod and a Ag/AgCl electrode saturated with KCl were used as a counter electrode and a reference electrode, respectively. The reference electrode was calibrated with respect to reversible hydrogen electrode (RHE). Impedance measurements were carried out at an overpotential of 0.3 V from 10^6 to 0.01 Hz with an AC voltage of 5 mV.

dx.doi.org/10.1021/jz400507t | J. Phys. Chem. Lett. 2013, 4, 1227−1232

■ ASSOCIATED CONTENT

Supporting Information

AFM images of mechanically or chemically exfoliated MoS_2 sheets, XPS, Raman, and UV/vis spectra of MoS_2/Au hybrids, TEM and HRTEM images of MoS_2/Au hybrids, and polarization curves of WS_2/Au hybrids with excessive gold decoration. This material is available free of charge via the Internet at http://pubs.acs.org.

■ AUTHOR INFORMATION

Corresponding Author

*E-mail: jiaxing-huang@northwestern.edu.

Notes

The authors declare no competing financial interest.

■ ACKNOWLEDGMENTS

J.H. thanks the Alfred P. Sloan Research Foundation for a Fellowship, the Sony Corporation for a gift donation, and the NSF CAREER Award (DMR 0955612). J.K. gratefully acknowledges the support from the Ryan Fellowship and the Northwestern University International Institute for Nanotechnology. S.B. was supported by Basic Science Research Program through the National Research Foundation of Korea funded by the MEST (Project No. 2012-000181). We thank I. S. Kim and Y.-K. Huang for technical assistance and NUANCE and NU-MRSEC for the use of their facilities.

■ REFERENCES

(1) Wang, Q. H.; Kalantar-Zadeh, K.; Kis, A.; Coleman, J. N.; Strano, M. S. Electronics and Optoelectronics of Two-Dimensional Transition Metal Dichalcogenides. *Nat. Nanotechnol.* **2012**, *7*, 699−712.

(2) Li, T. S.; Galli, G. L. Electronic Properties of MoS_2 Nanoparticles. *J. Phys. Chem. C* **2007**, *111*, 16192−16196.

(3) Eda, G.; Yamaguchi, H.; Voiry, D.; Fujita, T.; Chen, M. W.; Chhowalla, M. Photoluminescence from Chemically Exfoliated MoS_2. *Nano Lett.* **2011**, *11*, 5111−5116.

(4) Xu, C.; Wang, X.; Zhu, J. W. Graphene−Metal Particle Nanocomposites. *J. Phys. Chem. C* **2008**, *112*, 19841−19845.

(5) Muszynski, R.; Seger, B.; Kamat, P. V. Decorating Graphene Sheets with Gold Nanoparticles. *J. Phys. Chem. C* **2008**, *112*, 5263−5266.

(6) Kamat, P. V. Graphene-Based Nanoarchitectures. Anchoring Semiconductor and Metal Nanoparticles on a Two-Dimensional Carbon Support. *J. Phys. Chem. Lett.* **2010**, *1*, 520−527.

(7) Kim, F.; Luo, J. Y.; Cruz-Silva, R.; Cote, L. J.; Sohn, K.; Huang, J. X. Self-Propagating Domino-Like Reactions in Oxidized Graphite. *Adv. Funct. Mater.* **2010**, *20*, 2867−2873.

(8) Lee, S. H.; Lee, D. H.; Lee, W. J.; Kim, S. O. Tailored Assembly of Carbon Nanotubes and Graphene. *Adv. Funct. Mater.* **2011**, *21*, 1338−1354.

(9) Xiang, Q.; Yu, J. Graphene-Based Photocatalysts for Hydrogen Generation. *J. Phys. Chem. Lett.* **2013**, 753−759.

(10) Lee, W. J.; Lee, J. M.; Kochuveedu, S. T.; Han, T. H.; Jeong, H. Y.; Park, M.; Yun, J. M.; Kwon, J.; No, K.; Kim, D. H.; et al. Biomineralized N-Doped CNT/TiO_2 Core/Shell Nanowires for Visible Light Photocatalysis. *ACS Nano* **2012**, *6*, 935−943.

(11) Lee, D. H.; Lee, W. J.; Lee, W. J.; Kim, S. O.; Kim, Y. H. Theory, Synthesis, and Oxygen Reduction Catalysis of Fe-Porphyrin-Like Carbon Nanotube. *Phys. Rev. Lett.* **2011**, *106*, 175502.

(12) Zhang, W. Y.; Demydov, D.; Jahan, M. P.; Mistry, K.; Erdemir, A.; Malshe, A. P. Fundamental Understanding of the Tribological and Thermal Behavior of Ag-MoS_2 Nanoparticle-Based Multi-Component Lubricating System. *Wear* **2012**, *288*, 9−16.

(13) Shahar, C.; Levi, R.; Cohen, S. R.; Tenne, R. Gold Nanoparticles as Surface Defect Probes for WS_2 Nanostructures. *J. Phys. Chem. Lett.* **2010**, *1*, 540−543.

(14) Cheng, F. Y.; Chen, J.; Gou, X. L. MoS_2−Ni Nanocomposites as Catalysts for Hydrodesulfurization of Thiophene and Thiophene Derivatives. *Adv. Mater.* **2006**, *18*, 2561−2564.

(15) He, Q. Y.; Zeng, Z. Y.; Yin, Z. Y.; Li, H.; Wu, S. X.; Huang, X.; Zhang, H. Fabrication of Flexible MoS_2 Thin-Film Transistor Arrays for Practical Gas-Sensing Applications. *Small* **2012**, *8*, 2994−2999.

(16) Rao, B. G.; Matte, H. S. S. R.; Rao, C. N. R. Decoration of Few-Layer Graphene-Like MoS_2 and $MoSe_2$ by Noble Metal Nanoparticles. *J. Cluster Sci.* **2012**, *23*, 929−937.

(17) Huang, X.; Zeng, Z.; Bao, S.; Wang, M.; Qi, X.; Fan, Z.; Zhang, H. Solution-Phase Epitaxial Growth of Noble Metal Nanostructures on Dispersible Single-Layer Molybdenum Disulfide Nanosheets. *Nat. Commun.* **2013**, *4*, 1444.

(18) Laursen, A. B.; Kegnaes, S.; Dahl, S.; Chorkendorff, I. Molybdenum Sulfides-Efficient and Viable Materials for Electro- and Photoelectrocatalytic Hydrogen Evolution. *Energy Environ. Sci.* **2012**, *5*, 5577−5591.

(19) Merki, D.; Hu, X. L. Recent Developments of Molybdenum and Tungsten Sulfides as Hydrogen Evolution Catalysts. *Energy Environ. Sci.* **2011**, *4*, 3878−3888.

(20) Merki, D.; Fierro, S.; Vrubel, H.; Hu, X. L. Amorphous Molybdenum Sulfide Films as Catalysts for Electrochemical Hydrogen Production in Water. *Chem. Sci.* **2011**, *2*, 1262−1267.

(21) Vrubel, H.; Merki, D.; Hu, X. L. Hydrogen Evolution Catalyzed by MoS_3 and MoS_2 Particles. *Energy Environ. Sci.* **2012**, *5*, 6136−6144.

(22) Frame, F. A.; Osterloh, F. E. CdSe−MoS_2: A Quantum Size-Confined Photocatalyst for Hydrogen Evolution from Water under Visible Light. *J. Phys. Chem. C* **2010**, *114*, 10628−10633.

(23) Voiry, D.; Yamaguchi, H.; Li, J.; Silva, R.; Alves, D. C. B.; Fujita, T.; Chen, M.; Asefa, T.; Shenoy, V.; Eda, G.; et al. Enhanced Catalytic Activity in Strained Chemically Exfoliated WS_2 Nanosheets for Hydrogen Evolution. **2012**, arXiv:1212.1513 [cond-mat.mtrl-sci].

(24) Bahl, O. P.; Evans, E. L.; Thomas, J. M. Identification and Some Properties of Point Defects and Non-Basal Dislocations in Molybdenite Surfaces. *Proc. R. Soc. London, Ser. A* **1968**, *306*, 53−65.

(25) Choi, H. C.; Shim, M.; Bangsaruntip, S.; Dai, H. J. Spontaneous Reduction of Metal Ions on the Sidewalls of Carbon Nanotubes. *J. Am. Chem. Soc.* **2002**, *124*, 9058−9059.

(26) Kong, B. S.; Geng, J. X.; Jung, H. T. Layer-by-Layer Assembly of Graphene and Gold Nanoparticles by Vacuum Filtration and Spontaneous Reduction of Gold Ions. *Chem. Commun.* **2009**, 2174−2176.

(27) Shin, H. J.; Choi, W. M.; Choi, D.; Han, G. H.; Yoon, S. M.; Park, H. K.; Kim, S. W.; Jin, Y. W.; Lee, S. Y.; Kim, J. M.; et al. Control of Electronic Structure of Graphene by Various Dopants and Their Effects on a Nanogenerator. *J. Am. Chem. Soc.* **2010**, *132*, 15603−15609.

(28) Popov, I.; Seifert, G.; Tomanek, D. Designing Electrical Contacts to MoS_2 Monolayers: A Computational Study. *Phys. Rev. Lett.* **2012**, 108.

(29) Lide, D. R. *CRC Handbook of Chemistry and Physics*, 75th ed.; CRC Press: Boca Raton, FL, 1994.

(30) Joensen, P.; Frindt, R. F.; Morrison, S. R. Single-Layer MoS_2. *Mater. Res. Bull.* **1986**, *21*, 457−461.

(31) Py, M. A.; Haering, R. R. Structural Destabilization Induced by Lithium Intercalation in MoS_2 and Related-Compounds. *Can. J. Phys.* **1983**, *61*, 76−84.

(32) Eda, G.; Fujita, T.; Yamaguchi, H.; Voiry, D.; Chen, M. W.; Chhowalla, M. Coherent Atomic and Electronic Heterostructures of Single-Layer MoS_2. *ACS Nano* **2012**, *6*, 7311−7317.

(33) Chang, Y. H.; Lin, C. T.; Chen, T. Y.; Hsu, C. L.; Lee, Y. H.; Zhang, W.; Wei, K. H.; Li, L. J. Highly Efficient Electrocatalytic Hydrogen Production by MoS_x Grown on Graphene-Protected 3D Ni Foams. *Adv. Mater.* **2013**, *25*, 756−760.

(34) Li, Y. G.; Wang, H. L.; Xie, L. M.; Liang, Y. Y.; Hong, G. S.; Dai, H. J. MoS_2 Nanoparticles Grown on Graphene: An Advanced Catalyst

for the Hydrogen Evolution Reaction. *J. Am. Chem. Soc.* **2011**, *133*, 7296−7299.
(35) Jaramillo, T. F.; Jorgensen, K. P.; Bonde, J.; Nielsen, J. H.; Horch, S.; Chorkendorff, I. Identification of Active Edge Sites for Electrochemical H_2 Evolution from MoS_2 Nanocatalysts. *Science* **2007**, *317*, 100−102.
(36) Hinnemann, B.; Moses, P. G.; Bonde, J.; Jorgensen, K. P.; Nielsen, J. H.; Horch, S.; Chorkendorff, I.; Norskov, J. K. Biomimetic Hydrogen Evolution: MoS_2 Nanoparticles as Catalyst for Hydrogen Evolution. *J. Am. Chem. Soc.* **2005**, *127*, 5308−5309.
(37) Fiechter, S. Defect Formation Energies and Homogeneity Ranges of Rock Salt-, Pyrite-, Chalcopyrite- and Molybdenite-Type Compound Semiconductors. *Sol. Energy Mater.* **2004**, *83*, 459−477.
(38) Yang, D.; Frindt, R. F. Li-Intercalation and Exfoliation of WS_2. *J. Phys. Chem. Solids* **1996**, *57*, 1113−1116.
(39) Maeda, K.; Domen, K. Photocatalytic Water Splitting: Recent Progress and Future Challenges. *J. Phys. Chem. Lett.* **2010**, *1*, 2655−2661.
(40) Kamat, P. V. Manipulation of Charge Transfer across Semiconductor Interface. A Criterion That Cannot Be Ignored in Photocatalyst Design. *J. Phys. Chem. Lett.* **2012**, *3*, 663−672.
(41) Xu, B. H.; Lin, B. Z.; Sun, D. Y.; Ding, C. Preparation and Electrical Conductivity of Polyethers/WS_2 Layered Nanocomposites. *Electrochim. Acta* **2007**, *52*, 3028−3034.